

LOCAL MASS/HEAT TRANSFER DISTRIBUTION ON SURFACES ROUGHENED WITH SMALL SQUARE RIBS

F. P. BERGER and K.-F., F.-L. HAU

Department of Nuclear Engineering, Queen Mary College, University of London,
Mile End Road, London E1 4NS, U.K.

(Received 23 October 1978 and in revised form 1 May 1979)

Abstract—An electrochemical analogue technique has been used to measure the mass-heat transfer distribution in pipes roughened with square small ribs. The rib pitch to height ratios were varied from 3 to 10, the Reynolds number from 1×10^4 to 2.5×10^5 and the Schmidt number from 1×10^3 to 7×10^3 . Measurements were made in regions with different degrees of flow development. Representative mass transfer distributions are given and discussed. It has been found that the mass transfer distributions are less non-uniform at higher Reynolds numbers and that they are virtually independent of the Schmidt number over a wide range of Sc .

NOMENCLATURE

A ,	surface area of the cathode;
$Ar(e^+)$,	momentum transfer roughness function;
C_b ,	bulk concentration of reacting species of ions;
d ,	diameter of pipe (at rib root);
D ,	diffusion coefficient;
e ,	rib height;
$e^+ = eU^*/\nu$,	dimensionless rib height;
f ,	friction factor;
F ,	Faraday constant;
$G(e^+)$,	heat transfer roughness function;
I_L ,	limiting current;
K ,	mass transfer coefficient;
L ,	length of rough upstream section;
n_e ,	valency change of reacting ion species;
p ,	rib pitch;
u ,	local velocity;
U ,	mean flow velocity;
w ,	rib width;
x ,	distance downstream of rib;
ν ,	kinematic viscosity;
Re ,	Reynolds number, Ud/ν ;
Sc ,	Schmidt number, ν/D ;
St ,	Stanton number, K/U .

Subscripts

D ,	downstream;
R ,	rough mean;
R, x ,	rough local;
s ,	smooth;
U ,	upstream.

INTRODUCTION

SURFACES roughened with discrete small square ribs have been widely used for improving heat transfer from the fuel pins of gas-cooled nuclear reactors, less frequently in other applications. A large amount of

work has been done on experimental and semi-theoretical studies of the mean values of heat transfer (Stanton number) and friction factor on such surfaces, and this work has been comprehensively surveyed [1, 2]. The flow and turbulence patterns over such surfaces have also been studied in some detail [3-5]. However, relatively little has been done on the distribution of local heat transfer coefficients on such surfaces, probably because accurate measurements of this kind are rather difficult.

A good knowledge of the heat transfer distribution on and between the ribs is desirable for two main reasons. First of all it will improve our understanding of the mechanism by which the ribs actually influence heat transfer. Thus it will further theoretical approaches to the problem which so far have not been very successful. The second reason is a practical one. The heat rating of a reactor fuel element is often limited by the maximum temperature of the element's cladding. The actual surface temperature of the cladding varies to some extent over each rib-pitch depending on the heat transfer distribution and on the thermal conductivity of the cladding material. Codes exist for the calculation of the temperature micro-distribution [6] but they suffer from the lack of reliable data for the local heat transfer distribution. The problem may not be too serious in present thermal reactors but would be more significant in gas-cooled fast reactors with their high heat rating and stainless steel claddings.

Direct heat transfer experiments of this type are very difficult because of problems connected with the thermal insulation of small sections of the surface and with accurate measurements of the local heat flux and surface temperature. Therefore, virtually all previous investigators used some kind of mass transfer technique assuming the validity of the mass-heat transfer analogy. Two basic techniques have been employed—one based on the non-uniform sublimation of a naphthalene layer [7, 8], the other on the evaporation of water from absorbent paper

covering the ribbed surface [9]. Both methods suffer from drawbacks—in the first method the characteristics of the surface will be affected by the non-uniform wear of the naphthalene layer, in the second capillarity effects in the paper have an effect similar to that of the thermal conductivity in heat transfer experiments. In each of the few experiments that have been reported measurements were taken at one Reynolds number only; all were done at low Schmidt numbers.

For these reasons an experimental study was undertaken to determine local heat transfer distributions on the inner surface of a tube roughened with square sharp edged ribs in conditions of turbulent flow. This rib shape affects heat transfer performance more than most others and is widely used on nuclear fuel elements. The rib pitch to height ratio was varied from $p/e = 3$ to $p/e = 10$, thus covering the range most relevant for reactor applications and linking up with previous experiments at the same laboratory [4, 10, 11]. The ratio of rib height to tube diameter was kept constant at $e/d = 0.0364$. In the experiments an electrochemical analogue method was used which has been successfully applied in a number of other applications [12]. It is believed to be free from the mentioned drawbacks of other techniques and has other advantages as well. The main aims of the study were as follows: to verify the suitability of the electrochemical method for this type of measurement; to obtain reliable and accurate data for the local mass-heat transfer distribution over a wide range of Reynolds numbers, in particular for $p/e = 10$ but also for other p/e ratios; and to investigate the possible effect of Schmidt-Prandtl number variations on the distribution.

EXPERIMENTAL TECHNIQUE AND APPARATUS

In the experiments the well known system consisting of an aqueous solution of potassium ferri- and ferrocyanide with NaOH as the inert electrolyte was used as the flow medium. The principle advantages and limitations of the method have been discussed by the authors in some detail in a previous paper [13]. Here it will suffice to say that the method is particularly suitable for local measurements because the electrical insulation of small sections of the surface is easy (the applied potentials are very low, typically 1 V), and the quantity analogous to the heat flux (an electrical current) can be measured with high accuracy.

The experimental rig was the same as used in our previous experiments and has been described in [13, 14]. Four different measuring sections were used, each with a different p/e ratio, i.e. $p/e = 10, 7, 5, 3$ respectively. All of them had a rib root diameter of 110 mm and the rib width was always equal to the rib height, $w = e = 4$ mm. The first of these sections ($p/e = 10$) is shown in Fig. 1(a). It was composed of 10 ring-shaped nickel electrodes, each 3–3.5 mm wide, one of which formed the rib tip and the remaining 9 the surface between 2 ribs; the electrodes were separated by insulating UPVC rings. The other three measuring sections each consisted of two rib pitches as shown in Fig. 1(b) for $p/e = 7$. Again 3 mm wide electrodes with insulating rings formed the two rib tips, however the surface between the first and second rib was formed by a continuous ring electrode, and the section between the 2nd and 3rd rib was divided into 6 electrodes. The design of the measuring sections for the smaller pitch to height ratios was quite similar, only the number of electrodes between the second and third rib was

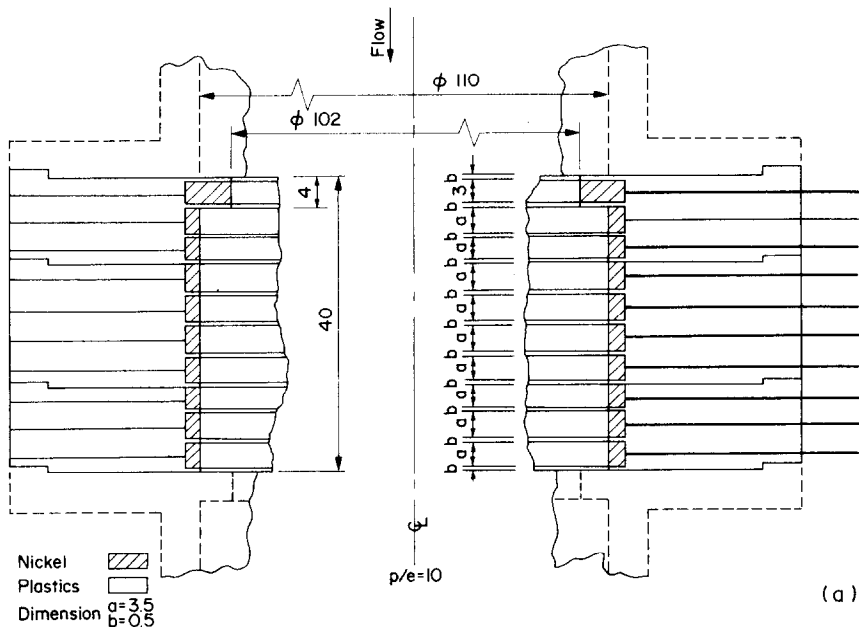


FIG. 1. (a) Measuring section with $p/e = 10$.

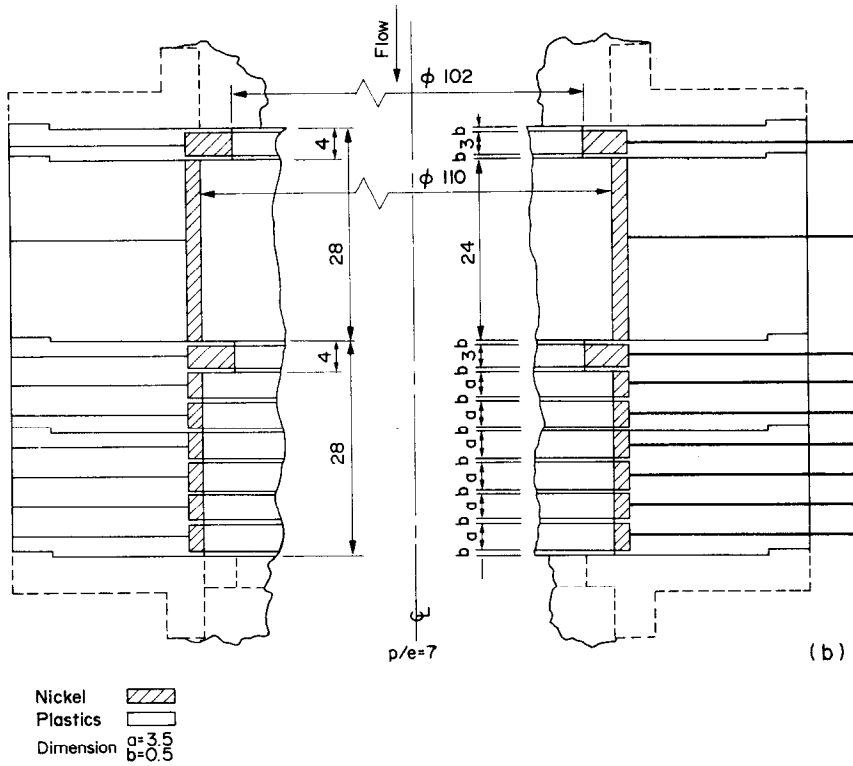


FIG. 1. (b) Measuring sections with $p/e = 7$.

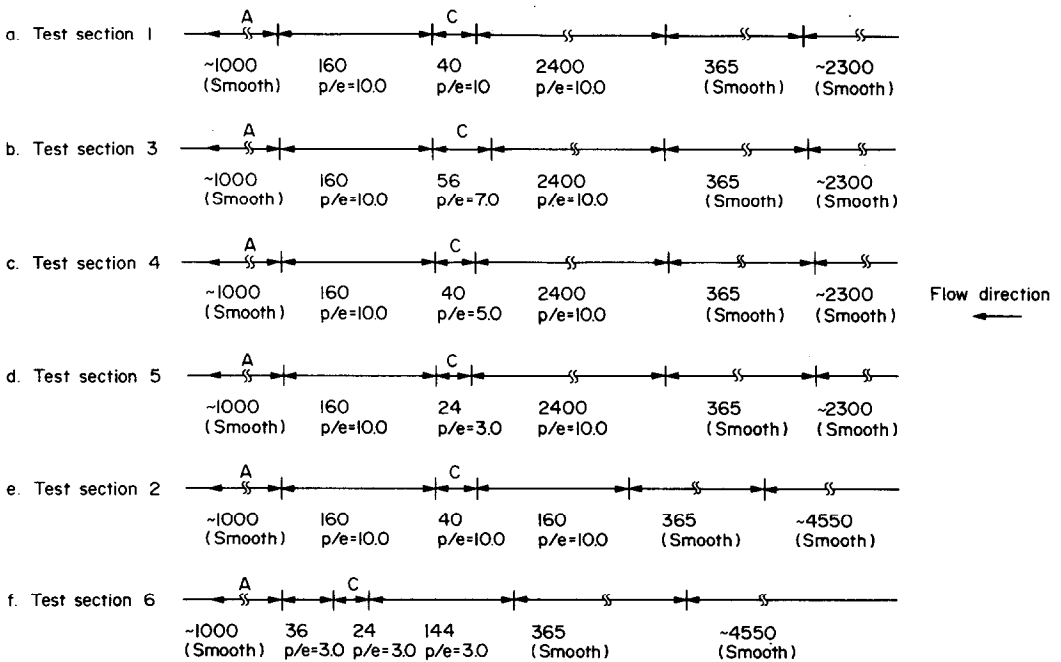


FIG. 2. Schematic arrangement of the six test sections. C = cathodes, A = anode.

correspondingly smaller (4 for $p/e = 5$; 2 for $p/e = 3$). The assembled measuring sections were polished in order to remove any unevenness or micro-roughness on the surface.

The measuring sections were variously combined with three different upstream and two different downstream sections, so that 6 different test sections (TS) were obtained; these are shown diagrammatically in Fig. 2. All the upstream and downstream sections were made from perspex and had the same inner diameter and rib dimensions as the measuring sections; they differed, however, in length and rib pitch. The first upstream section was 2.4 m long ($L/d \approx 23$) and had a rib pitch $p/e = 10$; it was used in combination with all four measuring sections (TS 1, 3, 4, 5). It has been proved in earlier experiments [10] that an L/d ratio of 23 is sufficient for full flow development in a rough pipe. Thus in test section 1 the flow in the measuring section may be assumed as fully developed. The same cannot be said of TS 3, 4 and 5, since here the rib pitch in the measuring section differed from that upstream of it. The second upstream section again had a ratio of $p/e = 10$ but contained only 4 ribs and was 160 mm long ($L/d \approx 1.5$); it was used in TS 2 together with the measuring section having $p/e = 10$. The conditions in the measuring section therefore corresponded to an early stage in flow development. The third upstream section had a rib pitch $p/e = 3$, contained 12 ribs and was 144 mm long ($L/d \approx 1.3$); it was used in TS 6 together with the measuring section having $p/e = 3$. The roughened downstream test section in TS 1–5 was 160 mm long and had a ratio $p/e = 10$; in TS 6 the downstream section was only 36 mm long and had $p/e = 3$.

The term 'fully developed' implies that in the bulk of the flow the x -wise velocity gradient $du/dx = 0$. In the immediate vicinity of the surface flow, contraction and expansion occurs on each rib pitch and du/dx will, therefore, always vary with x . It has been shown in other experiments [4] that the region where $du/dx = f(x)$ extends to a distance of about two rib heights above the rib tip. In view of the high Schmidt numbers in the present experiments, the concentration boundary layer is much thinner than the region of variable du/dx . Hence one would expect that the development of the mass transfer coefficient will be governed by the development of the velocity profile and it was deemed sufficient to use the short active measuring sections described before. Indeed tests on the section with two rib pitches have shown that the readings on the second pitch do not change when the first pitch is disconnected from the electrical circuit.

In all cases a smooth nickel tube (I.D. = 102 mm, length 1 m) was placed below the downstream section and was used as the anode.

The flow through the test sections was always downwards. The elements of the test sections were centred and sealed with O-rings and the whole assembly was held together by three long tie-rods. Great care was taken to ensure straightness of the test

sections and to avoid any discontinuities or steps on the inner surface. The straight length in front of each measuring section was about 50 tube diameters, so that any effect of the upper bend could be neglected.

All the cathodes and the anode were permanently connected to a continuously variable stabilised power supply but the current on each of the cathodes was measured separately with an accuracy of $\pm 0.5\%$. The current–voltage curves were plotted with the help of an X–Y recorder and the limiting current I_L was found from this curve. The mass transfer coefficient K was then calculated from the well known formula

$$K = \frac{I_L}{n_e F A C_b} \quad (1)$$

The electrolytic aqueous solution employed as the flow medium contained 0.002–0.005 M potassium ferricyanide $K_3Fe(CN)_6$, 0.005–0.01 M potassium ferrocyanide $K_4Fe(CN)_6$ and 1.0–4.0 M sodium hydroxide NaOH. High purity chemicals and demineralized water were used for its preparation. It has been pointed out earlier [13] that it is beneficial to work with lower ferricyanide concentrations because this helps to ensure that the reaction on the cathode is the controlling one, and also because the effect of the ohmic resistance on the results is reduced. The Schmidt number is controlled by the NaOH concentration and by the temperature of the solution—in the given case Sc was varied in the range 1000–7000. The concentration of the cyanides was determined by titration methods with an accuracy not worse than $\pm 1.2\%$. The experimental and activation procedure was essentially the same as described in [13].

The flow rate through the test section was controlled by throttling in the outlet pipe from the pump and was measured with two alternative orifices. The temperature of the fluid was kept constant by a thermostat-controlled cooler coil in the tank. The tests were carried out at Reynolds numbers ranging from 1×10^4 to 2.5×10^5 .

EXPERIMENTAL RESULTS AND DISCUSSION

Test section with $p/e = 10$

The measured local mass transfer coefficients $K_{R,x}$ were normalized by the value of the mean mass transfer coefficient K_s which would obtain in a smooth pipe at the same values of Re and Sc . The values of K_s were calculated from a formula, derived from earlier tests with smooth pipes [13]

$$K_s = 0.0165U Re^{-0.14} Sc^{-0.67}, \quad (2)$$

where U is the mean flow velocity.

Figure 3 shows the normalized local mass transfer coefficients on the surface with $p/e = 10$ for fully developed flow conditions and varying Reynolds numbers. It is seen that the curves have three maxima and 2 minima. The first and highest maximum is on the rib tip. This is immediately followed by a deep

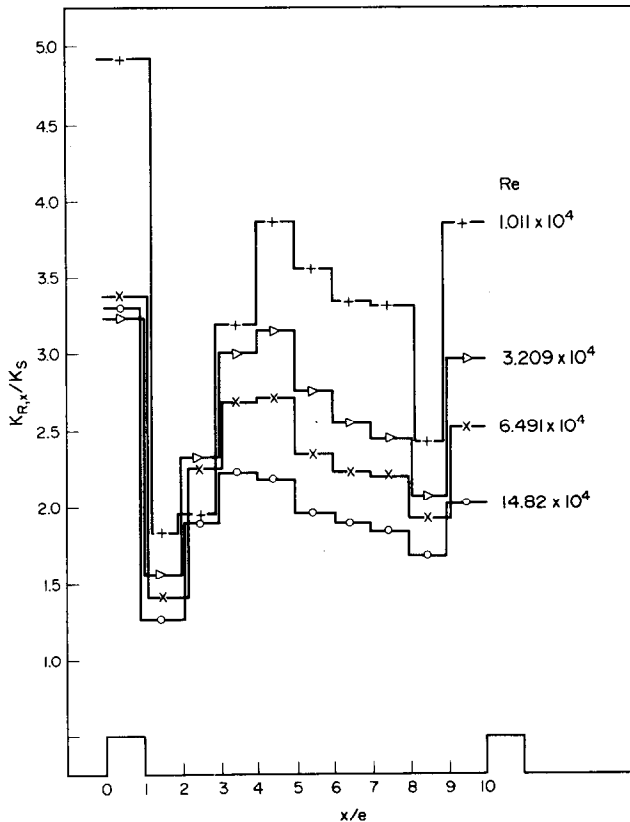


FIG. 3. Mass transfer coefficient distribution in fully developed flow for $p/e = 10$ at $Sc = 1535$.

minimum in the wake of the rib, but at all Reynolds numbers the value of $K_{R,x}$ at this point is still higher than K_s in a smooth pipe. With increasing distance from the rib, $K_{R,x}$ increases again until the second maximum is reached at three to four rib heights downstream of the rib; the distance decreases with increasing Re . It is believed that the position of this maximum more or less coincides with the reattachment point of the separated flow. Indeed its position agrees very well with the reattachment points found by wind-tunnel measurements on similar surfaces at the same laboratory [4] (3.2 rib heights downstream of the rib for $Re > 10^5$). The position of the maximum also agrees reasonably well with that found by other investigators [4, 8, 9]. With x increasing further, the boundary layer starts developing and the mass transfer coefficients fall again until the second minimum is reached one to two rib heights upstream of the next rib; the value of $K_{R,x}$ at this point is always higher than in the immediate wake. Just in front of the next rib a third maximum, similar in value to the second, is observed. It is believed that this maximum is caused by flow separation and eddying. Apart from the shift in position of the second maximum the Reynolds number does not seem to have much effect on the general shape of the mass transfer distribution. It is, however, seen that as Re increases the

curve becomes flatter and the values of $K_{R,x}/K_s$ generally decrease. This implies that at these high Schmidt numbers the improvement in heat transfer caused by the roughnesses is smaller at higher Reynolds numbers. In other words, the mean mass transfer coefficient K_R is a stronger function of Re than K_s , given by equation (2); this is shown in Fig. 4. In this respect the relative change of the K_R and K_s values differs from that in the low Schmidt (or Prandtl) number range where the variation of K_R/K_s with Re is very small. On the other hand, for a given Reynolds number, the values found for $K_{R,x}/K_s$ at higher Schmidt numbers (up to $Sc = 7200$) were quite similar to those in Fig. 3. It follows that at least in the tested range of Sc the dependence of K_R on Sc is the same as that of the smooth K_s , and also that the dependence of K_R on Re in this Schmidt number range can be expressed as a power function with a constant exponent on Re . It was found that the experimental results were well represented by the equation

$$St_R = 0.281 Re^{-0.305} Sc^{-0.67}, \quad (3)$$

the deviations being within $\pm 5.5\%$.

The mean mass transfer coefficient in St_R was calculated from the measured local values on the rib tip and between the ribs, as if the total surface area were equal to the surface area of a smooth pipe with the

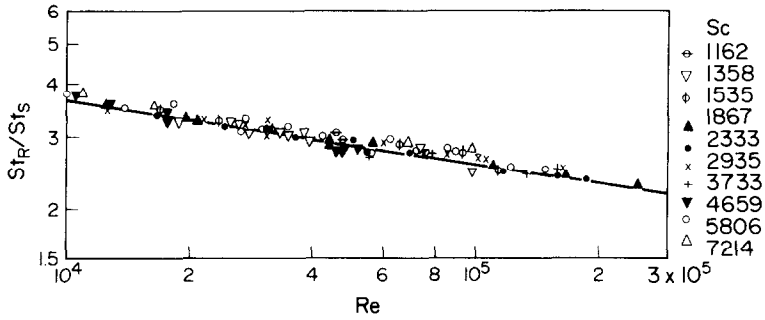


FIG. 4. Normalized mean Stanton number vs Reynolds number for $p/e = 10$ in fully developed flow at different Schmidt numbers.

rib root diameter. This is an approach often used in the evaluation of St_R . It is implicitly assumed in this method of calculating St_R that the local mass transfer coefficients on the sides of the rib (which were not measured in the present study) are equal to the mean value over the surface. This assumption is supported by the experiments of Katchee and Mackewicz, and for the surface with $p/e = 10$ the error caused by it will in all probability be very small. However, for smaller p/e ratios the relative importance of the side walls of the rib increases and measurements of the mass transfer on these sides will be made in the near future.

Figure 5 shows a comparison of the present distribution (this time expressed as the ratio of the local to the mean value of the mass transfer coefficient

on the rough surface) with that of Katchee and Mackewicz [7] for very similar values of p/e and Re . Also included are the data of Walker and Wilkie [8] obtained at higher values of p/e and Re . The agreement is generally reasonable, the positions and values of the maxima agree particularly well. Walker's third maximum is naturally further downstream because of the higher p/e , but its value appears to be abnormally high, perhaps due to the technique used. Since all previous measurements were done at low Schmidt numbers ($Sc \approx 1$) it appears that the distribution of the normalized mass transfer coefficient ($K_{R,x}/K_R$) is independent of Sc over a very wide range of Schmidt or Prandtl numbers.

Figure 6 shows a comparison of the measured $K_{R,x}$

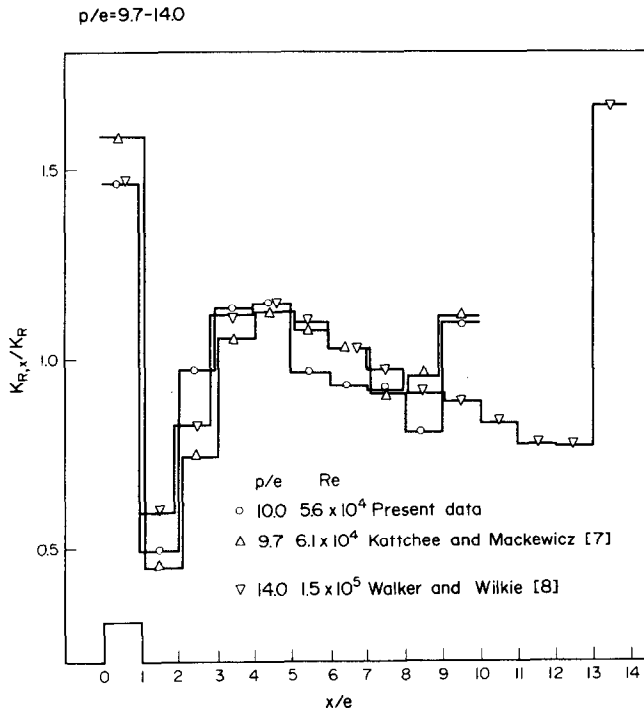


FIG. 5. Comparison of mass transfer coefficient distributions with those obtained by other investigators.

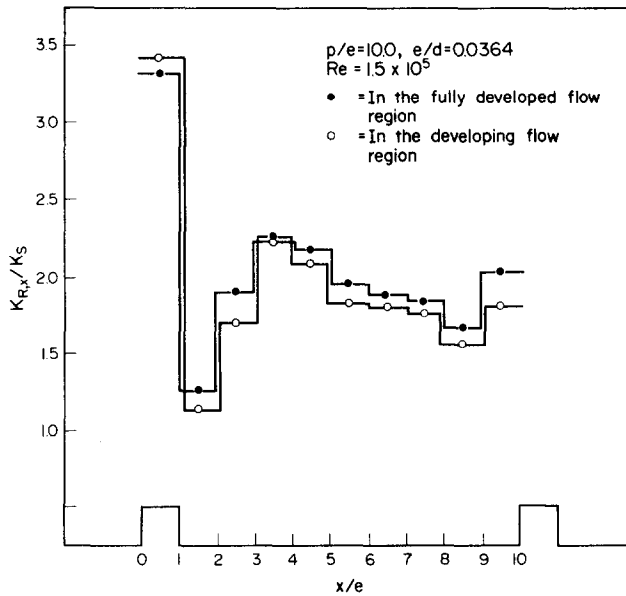


FIG. 6. Comparison of mass transfer coefficients in the developing and fully developed flow regions. ($p/e = 10, Re = 1.5 \times 10^5, Sc = 1535$).

in the fully developed region (TS 1) and in the developing regions (TS 2). It is seen that already after 4 rib pitches from the start of roughening the curves are very similar to those for fully developed flow; the local $K_{R,x}$ is slightly higher on the rib tip but slightly lower over most of the surface between the ribs; the mean K_R is about 5% lower than in the fully developed flow.

Since the dependence of St on Re is generally different at very high and low Schmidt or Prandtl numbers, equation (3) should not be used directly for predicting St_R for the case of heat transfer at low Pr , and some transformation is required. In order to establish how the present results can best be applied to the low Pr range, data obtained by Whitehead [2] and Webb [16] in heat transfer tests in similar geometries were used for comparison. It was found that good agreement was achieved by using the correlation suggested by Leslie [17]

$$(1/St_R) = (2/f_R) + \sqrt{(2/f_R)} [G(e^+)F(Pr) - Ar(e^+)] + P + Q\sqrt{(f_R/2)}, \quad (4)$$

where $P = 18.2, Q = 15.5$.

Since the friction factor was not measured in the present tests, f and Ar were calculated from expressions given by Whitehead, (these quantities are obviously not affected by the value of Pr)

$$\sqrt{(2/f_R)} = 2.44 \ln(d/2e) - 4.5 + Ar(e^+), \quad (5)$$

$$Ar(e^+) = 6.53(p/e)^{-0.24}. \quad (6)$$

For the case of high Schmidt numbers the term $\sqrt{(2/f_R)} [G(e^+)F(Pr)]$ in equation (4) is very much larger than all the other terms on the right hand side

and can be calculated directly from equation (3). The equation used for transformation can then be written as

$$(1/St_R)_{Pr} = (1/St_R)_{Sc}(Pr/Sc)^{0.67} + (2/f_R) + P + Q\sqrt{(f_R/2)} - \sqrt{(2/f_R)} Ar(e^+), \quad (7)$$

where $(1/St_R)_{Sc}$ corresponds to the presently measured St_R at high Schmidt numbers, $(1/St_R)_{Pr}$ corresponds to the value of St_R in heat transfer at low Pr .

The maximum deviations of Whitehead's experimental data from the values predicted in this way was less than 10%. Webb's data exhibit a larger deviation (up to 20%) but this discrepancy is due to the generally lower value of f_R found by Webb.

Test sections with $p/e = 7, 5$ and 3

The mass transfer distribution on the surface with $p/e = 7$ is shown in Fig. 7. As mentioned before the upstream section had in this case a pitch to height ratio $p/e = 10$ and the flow in the measuring section may, therefore, not be fully developed. However, because of the known similarity of behaviour of surfaces with those two p/e ratios and in view of the observed similarity in behaviour of the fully developed and developing regions in the case of $p/e = 10$ (see Fig. 6), the observed profile is in all probability very similar to that in the fully developed region. The distribution is indeed similar to that in Fig. 5 ($p/e = 10$), the main difference being that the third maximum is now even higher than the second. This may perhaps be caused by the relative proximity of the two maxima; the low between them is very short and shallow because of the shorter rib pitch. The data are again in reasonable agreement with those of [7] and [8] who tested surfaces with $p/e \approx 8$.

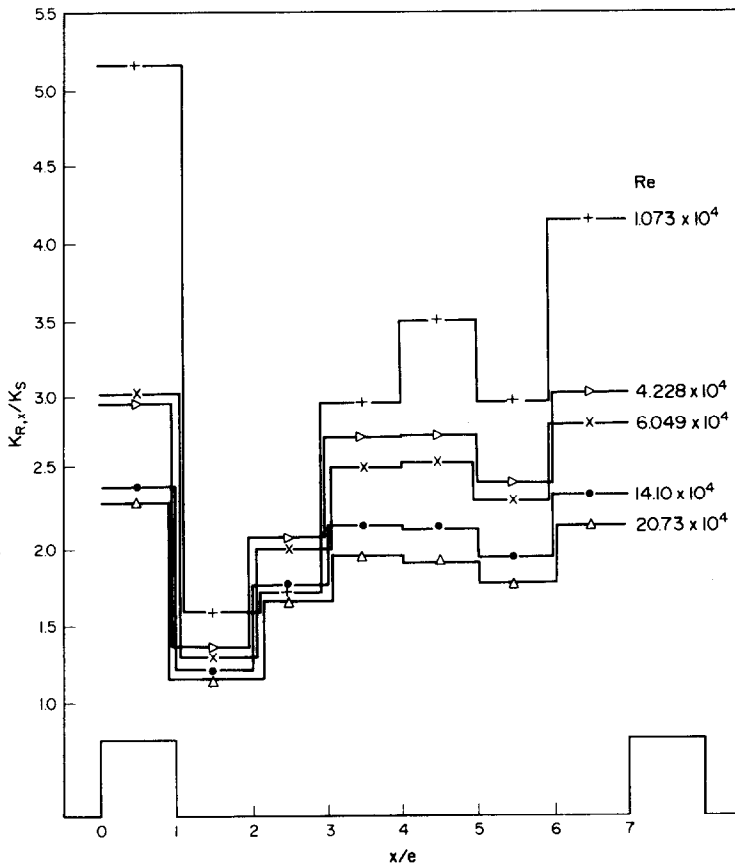


FIG. 7. Mass transfer coefficient distributions in measuring section with $p/e = 7$; $Sc = 1566$.

The behaviour of the two surfaces with small p/e ratios is different. Figure 8 shows that for $p/e = 5$ there is again a high maximum on the rib tip followed by a minimum in the wake. A second unusually high maximum appears immediately in front of the next rib; the value of $K_{R,x}$ at this point is even slightly higher than on the rib tip. Obviously in this case flow reattachment and flow separation occur very close together and this produces locally very favourable conditions for mass and heat transfer.

The behaviour of the surface with $p/e = 3$ in both its arrangements is shown in Fig. 9. The dashed lines are those from the arrangement with the long upstream section having $p/e = 10$ (TS 5), the full lines are those obtained with the short upstream section having $p/e = 3$ (TS 6). With the narrow rib spacing of $p/e = 3$ reattachment should not occur and one would expect that the flow will skim over the surface with standing vortices filling the space between the ribs, and that the values of $K_{R,x}$ will be relatively low. Contrary to these expectations in both cases a pronounced maximum is found in front of the second rib. However in TS 6 all local values of $K_{R,x}$ are lower than in TS 5, and the difference is largest in the position of the second maximum. This may be due on the one hand to the

different conditions on the inlet to the measuring section and on the other hand to the higher degree of flow development in TS 6.

Williams and Watts in their experiments with square ribs with $p/e = 3$ also found that the mass transfer coefficient between the ribs was highest in front of the second rib, but their actual values of $K_{R,x}$ over a substantial part of this surface were lower than that for a smooth tube. This discrepancy may well be due to the low degree of flow development in the present experiments.

Table 1 provides further information on this point. It gives the mean values of the Stanton number $St_R = K_R/U$ obtained on the first ($St_{R,U}$) and second pitch ($St_{R,D}$) of the measuring sections with $p/e = 3$ (both arrangements), $p/e = 5$ and $p/e = 7$. The values of $St_{R,U}$ and $St_{R,D}$ were calculated from the arithmetic mean of $K_{R,x}$ excluding the rib tip. The data for both measuring sections with $p/e = 3$ show that the downstream $St_{R,D}$ is lower than $St_{R,U}$. The difference between the two values is larger in the case of TS 6 (short upstream section with $p/e = 3$), especially at high Reynolds numbers. Thus it appears that in the inlet section of a pipe roughened with ribs having $p/e = 3$ the mass transfer coefficient decreases with

increasing distance from the entrance, quite similarly to the behaviour in a smooth pipe. However, the results from TS 5 (long upstream section with $p/e = 10$) are probably strongly influenced by the highly turbulent flow in the upstream section.

A comparison of the two pitches of the measuring section with $p/e = 5$ shows a similar behaviour. Again $St_{R,D}$ is lower than $St_{R,U}$ and the difference at low Re is more significant ($\sim 7\%$) than at high Re ($Re > 10^5$) when it amounts to only 2–3%.

However, the behaviour of the surfaces with the other two p/e ratios is different. For $p/e = 7$ the downstream pitch has a higher mean mass transfer coefficient than the upstream one. A similar observation on the test section with $p/e = 10$ has already been mentioned. Thus it appears that in the entrance section of pipes roughened with square ribs having $p/e \geq 7$ the mass–heat transfer coefficient increases with increasing x until the fully developed value is reached, whereas for $p/e \leq 5$ the opposite is

true. These findings are in qualitative agreement with those of Edwards and Sheriff [15] who roughened their surfaces with strung wires.

For a complete picture of the variations of the mean K_R in the entrance section of pipes with different p/e ratios it is necessary to carry out more extensive tests over the whole length of developing flow. Considering the differing effects at different p/e ratios conclusions should not be drawn from the present data as to the mean values of the mass–heat transfer coefficients in fully developed flow for ratios different from $p/e = 10$. The present tests imply that very near the entrance the variation of K_R with p/e can be substantially different from that in fully developed flow.

Nevertheless, the distributions of the local mass transfer coefficients found for $p/e = 7$ and also for $p/e = 3$ are in all probability representative of the distributions in fully developed flow. In the case of $p/e = 5$ complementary tests are required to confirm the observed distribution.

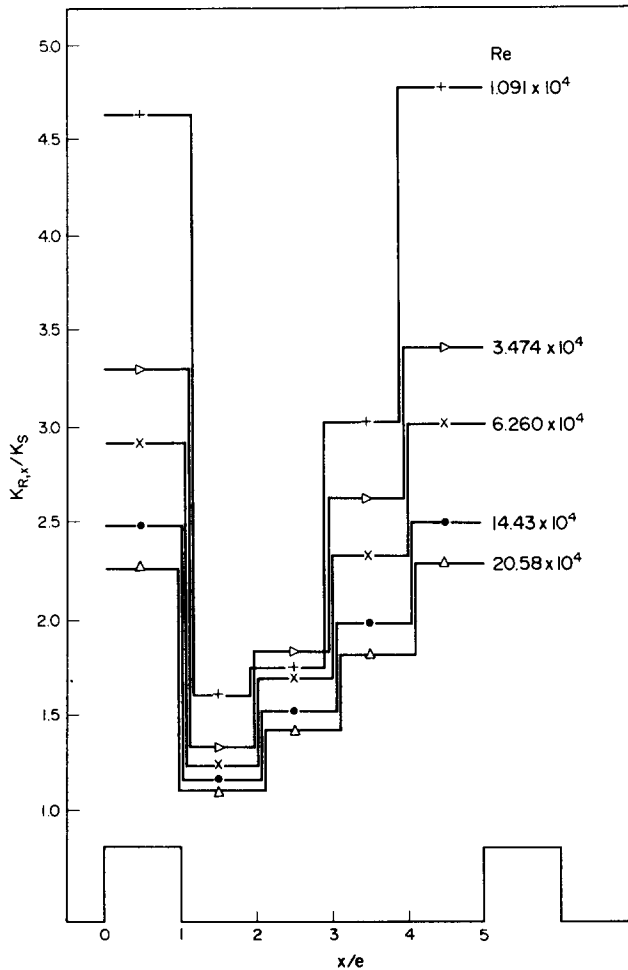


FIG. 8. Mass transfer coefficient distributions in measuring section with $p/e = 5$; $Sc = 1445$.

- Δ \circ ∇ Short rough entrance section (test section 6)
 \blacktriangle \bullet \blacktriangledown Long rough entrance section (test section 5)

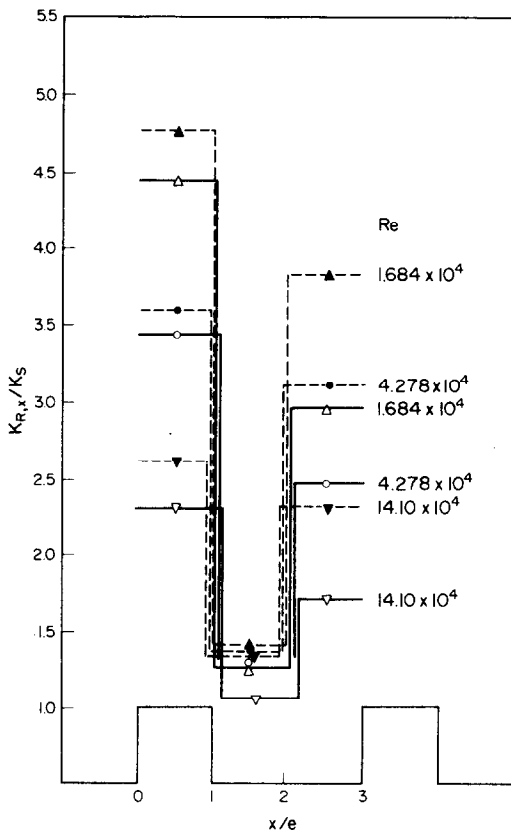


FIG. 9. Mass transfer coefficient distributions in the measuring section with $p/e = 3$ for the two different inlet conditions. $Sc = 1535$ in both cases.

CONCLUSIONS

1. It has been shown that the electrochemical analogue technique is a useful and convenient tool for investigating local and mean transfer values on rough surfaces.

2. Local mass transfer distributions have been established for surfaces roughened with square ribs with $p/e = 10$ in fully developed flow, and also in the region of developing flow. For the given p/e ratio, the distribution after 4 rib pitches is already very similar to that in fully developed flow and so is the mean mass-heat transfer coefficient.

3. Mass transfer distributions have been obtained for $p/e = 7, 5$ and 3 in the region of developing flow, and in the case of $p/e = 3$ for two different inlet conditions. The results indicate that the change in the mean Stanton number with distance from inlet has a different character for $p/e \geq 7$ and for $p/e \leq 5$.

4. In all cases the variations in the local mass transfer coefficients along one rib pitch are smaller at

higher Reynolds numbers. The reduction in the mean Stanton number with increasing Re is larger than for a smooth surface.

5. In the tested range of Schmidt numbers ($Sc = 1000-7000$) the relative local mass transfer distributions ($K_{R,x}/K_R$) are independent of Sc . The similarity of the present curves to those obtained by other investigators at low Sc numbers implies that the relative distributions obtained with the electrochemical method are representative even for low Sc , at least in fully developed flow over roughnesses with $p/e = 10$.

6. It has been shown for the case of $p/e = 10$ that from the mean Stanton number obtained by the electrochemical method (high Sc) it is possible to predict with fair accuracy the corresponding St in heat transfer at low Pr , provided that the friction factor and roughness function of the surface are known or measured.

7. Further work is required to establish the local transfer distributions in fully developed flow for p/e ratios smaller than 10, and to verify their applicability to the case of low Schmidt numbers.

REFERENCES

- M. Dalle Donne and L. Meyer, Turbulent convective heat transfer from rough surfaces with two dimensional rectangular ribs, *Int. J. Heat Mass Transfer* **20**, 583-620 (1977).
- A. W. Whitehead, The effects of surface roughening on fluid flow and heat transfer. Ph.D. Thesis, Queen Mary College, University of London (1976).
- J. Hanjalic and B. E. Launder, Fully developed asymmetric flow in a plane channel, *J. Fluid Mech.* **51**, 301-335 (1972).
- A. Aytakin and F. P. Berger, Turbulent flow in rectangular ducts with low aspect ratios having one rough wall, *Nuclear Energy* **18**, 53-63 (1979).
- W. Baumann, Geschwindigkeitsverteilung bei turbulenter Stroemung an rauhen Waenden, Report KfK 2618, April (1978).
- P. G. Barnett, The influence of wall thickness, thermal conductivity and method of heat input on the heat transfer performance of some ribbed surfaces, *Int. J. Heat Mass Transfer* **15**, 1159-1169 (1972).
- N. Kattchee, W. V. Mackewicz, Effects of boundary layer turbulence promoters on the local film coefficients of ML-1 fuel elements, *Nuclear Sci. Eng.* **16**, 31-38 (1965).
- V. Walker and D. Wilkie, The wider application of roughened heat transfer surfaces developed for advanced gas-cooled reactors, *Proc. I.M.E. Symposium on High Pressure Gas as a Heat Transport Medium* Paper 26, 190-197 (1967).
- F. Williams and J. Watts, The development of rough surfaces with improved heat transfer performance; a study of the mechanism involved, *4th Int. Heat Transfer Conf. (Versailles)*, Paper FC 5, 4 (1970).
- F. P. Berger and A. W. Whitehead, Fluid flow and heat transfer in tubes with internal square rib roughening, *J. Brit. Nucl. Energy Soc.* **16**, 153-160 (1977).
- A. Aytakin, Turbulent flow and heat transfer in channels with combined rough and smooth surfaces. Ph.D. Thesis, Queen Mary College, University of London (1978).
- T. Mizushima, The electrochemical method in transport phenomena, *Adv. Heat Transfer* **7**, 87 (1971).

13. F. P. Berger and K.-F., F.-L. HAU, Mass transfer in turbulent flow measured by the electrochemical method, *Int. J. Heat Mass Transfer* **20**, 1185–1194 (1977).
14. K.-F., F.-L. HAU, Applications of an electrochemical analogue method in mass, heat and momentum transfer studies. Ph.D. Thesis, Queen Mary College, University of London (1978).
15. F. J. Edwards and N. Sheriff, The heat transfer and friction characteristics for forced convection air flow over a particular type of rough surface, *ASME. Int. Development in Heat Transfer Conf., Part 2 Paper* 48, 415 (1961).
16. R. L. Webb, Turbulent heat transfer in tubes having two-dimensional roughness, including the effect of Prandtl number. Ph.D. Thesis, Univ. of Minnesota (1969).
17. D. C. Leslie, The form of extended Reynolds analogy for rough surfaces, *Let. Heat Mass Transfer* **5**, 99–109 (1978).

HMT 680

DISTRIBUTION DU TRANSFERT LOCAL DE CHALEUR ET DE MASSE
SUR DES SURFACES RENDUES RUGUEUSES PAR DES PETITS
ANNEAUX CARRÉS

Résumé — Une méthode analogique électrochimique est utilisée pour mesurer la distribution du transfert de chaleur et de masse dans des tubes rendus rugueux par des petits anneaux carrés. Les rapports pas/hauteur des anneaux varient de 3 à 10, le nombre de Reynolds de 10^4 à $2,5 \times 10^5$ et le nombre de Schmidt de 10^3 à 7×10^3 . Les mesures sont faites à différentes étapes du développement de l'écoulement. Des distributions de transfert massique sont données et discutées. On trouve que les distributions de transfert massique sont moins non-uniformes aux nombres de Reynolds plus élevés et qu'elles sont virtuellement indépendantes du nombre de Schmidt pour un large domaine de celui-ci.

ÖRTLICHE WÄRME- bzw. STOFFÜBERGANGSVERTEILUNG AUF
OBERFLÄCHEN MIT KÜNSTLICHEN RAUHIGKEITEN IN FORM KLEINER
QUADRATRIPPEN

Zusammenfassung — Mit Hilfe einer elektrochemischen Analogietechnik wurde die Wärme- bzw. Stoffübergangsverteilung in Röhren, die mittels kleiner Quadratrippen rauh gemacht worden waren, gemessen. Das Verhältnis von Rippenabstand zu Höhe wurde im Bereich von 3 bis 10 variiert, die Reynolds-Zahl von 10^4 bis $2,5 \cdot 10^5$ und die Schmidt-Zahl von 10^3 bis $7 \cdot 10^3$. Messungen wurden in Bereichen unterschiedlicher Strömungsbildung gemacht. Typische Stoffübergangsverteilungen werden angegeben und diskutiert. Es zeigte sich, daß die Stoffübergangsverteilungen bei hohen Reynolds-Zahlen weniger ungleichförmig sind und daß sie über einen weiten Bereich von Schmidt-Zahlen von diesen praktisch nicht abhängen.

ЛОКАЛЬНОЕ РАСПРЕДЕЛЕНИЕ ТЕПЛО- И МАССОБМЕНА ПО ПОВЕРХНОСТЯМ
С НЕБОЛЬШИМИ КВАДРАТНЫМИ РЕБРАМИ

Аннотация — Для измерения распределения тепла и массы в трубах с небольшими квадратными ребрами использован метод электрохимической аналогии. Отношение шага к высоте ребра изменялось в пределах от 3 до 10, число Рейнольдса — от 1×10^4 до $2,5 \times 10^5$, число Шмидта — от 1×10^3 до 7×10^3 . Измерения проводились в областях с различными степенями развития потока. Приведены характерные распределения массопереноса и дан их анализ. Найдено, что распределения переноса массы менее неоднородны при более высоких числах Рейнольдса и что фактически они не зависят от числа Шмидта в широком диапазоне его изменения.